FEDERAL UNIVERSITY OF TECHNOLOGY, AKURE
JOURNAL OF ENGINEERING AND ENGINEERING TECHNOLOGY

DESIGN AND SIMULATION OF TURBOCHARGER-DERIVED MICROTURBINE SYSTEM FOR COMBINED HEAT AND POWER GENERATION

Mogaji, T. S.*, Egunbiyi, T. O. and Idowu, E. T.

Department of Mechanical Engineering, School of Engineering and Engineering Technology,
Federal University of Technology,Akure, Ondo State, Nigeria

Mogaji, T. S., Egunbiyi, T. O. and Idowu, E. T. (2023): Design and Simulation of Turbocharger-derived Microturbine System for Combined Heat and Power Generation *Journal of Engineering And Engineering Technology /17(1), 91-101*

Received Date: 15-03-23 **Acceptance Date:22-06-23**

Abstract
In this study, an analytical design and numerical simulation of components of turbocharger-derived microturbine co-generator was carried out to assess the feasibility or workability of a turbo-charger derived microturbine for combined heat and power generation. A simple gas turbine or Brayton cycle was modeled analytically as the working cycle and validated with GasTurb13. An external combustion chamber of Tubo-annular type was adopted and modeled. The combustion characteristic was simulated using ANSYS Fluent 2021R1. A tube-in-tube heat exchanger was selected as the heat recovery unit, modeled and simulated using ANSYS Fluent 2021R1. Theoretical predictions with less than 3% variation in the outlet temperature of the designed system heat exchanger component is found closely matched with the numerical simulation results obtained in this study. Other simulation results carried out showed that the design is considered safe and fit for fabrication. The system when fabricated can be used for heat and power generation efficiently as designed for.

Keywords: *Design, simulation, turbocharger-derived microturbine, heat and power generation*

NOMENCLATURES

Parameter	Unit
Ambient pressure, P_1	Pa
Ambient temperature, T_1	K
Turbine outlet Temperature, T_4	K
Compressor pressure ratio, r_c	
Compressor efficiency, η_c	
Turbine efficiency, η_t	
Turbine pressure ratio r_t	
Compressor outlet temperature, T_2	K
Turbine inlet temperature, T_3	K
Specific heat capacity of fuel (Butane), C_{pf}	kJ/kg
Mass flow rate of fuel, m_f	kg/s
Work done by compressor, W_c	kJ/kg
Work done by turbine, W_t	kJ/kg
Ne work done, W_{net}	kJ/kg
Shaft output power, P	$kWatts$
Specific fuel consumption, SFC	kg/kWh
Pressure loss factor, q_{ref}	

Reference area, A_{ref}	m^2
Cross sectional area of the flame tube, $\frac{A_{ft}}{A_{ref}}$	
Total length of the flame tube, L_{ft}	M
Mass flow rate into primary zone, m_{pz}	kg/s
Mass flow rate into secondary zone, m_{sz}	kg/s
Mass flow rate into dilution zone, m_{dz}	kg/s
Air mass in the primary zone axially, $m_{pz-axial}$	kg/s
Velocity of jet in the annulus, U_j	m/s
Velocity of jet in the annulus, U_g	m/s
Admission hole properties in the primary zone, j	
Maximum penetration depth of air jet, Y_{max}	M
Diameter of the admission hole in the primary zone, d_h	M
Number of holes in the primary zone, n	
Diameter of the admission hole in the secondary zone, d_h	M
Number of holes in the secondary zone, n	
Cross sectional area of the required swirler, A_{sw}	m^2
Inner swirler diameter, D_{swin}	M
Outer swirler diameter, D_{sw}	M
Swirl number, S_N	
Swirl vane angle, θ	o
Divergent angle of dome, α_{dome}	o
length of required dome, L_{dome}	m
Expected turbine exit temperature, T_{hin}	$°C$
Room temperature of water, T_{cin}	$°C$
Desire final temperature of water, T_{cout}	$°C$
Selected mass flow rate of water, m_w	kg/s
Outlet temperature of water, T_{cout}	$°C$
Outlet temperature of the flue gas, T_{hout}	$°C$
Inner Copper tube internal diameter,	Cm
Copper tube thickness,	Cm
Outer copper tube internal diameter,	Cm
Reynold number of the flue gas in the inner tube, R_e	
Fictional factor, f	
Reynold number of the flue gas in the inner tube, R_e	
Fictional factor, f	
Nuselt number, Nu	
Heat transfer coefficient in the inner pipe, h_i	W/m^2K
Reynold number in annulus part, R_o	
Fictional factor, f	
Nuselt number, Nu	
Convective heat transfer coefficient in the annulus, h_o	W/m^2K
Logarithmic mean temperature difference, Δt	$°C$
Length of the heat exchanger, L	m
Overall heat transfer coefficient, U	W/m^2K

Introduction

Combined heat and power generation is a power generation and energy recovery method with the potential to provide efficient energy and environmental benefits by reducing primary energy consumption and associated greenhouse gas emission. Manabe, (2019) pointed out that as a direct consequence, the concentration of greenhouse gases has reached alarming levels, impacting onto the climate of our planet. This technology is aimed at providing solutions to technical and social problems that include the reduction of greenhouse gas emissions from energy supply, increased decentralization of energy supply, improved energy security, minimize energy losses from electrical transmission and distribution networks, and potentially reduced energy cost to consumers **(**Maryam *et al.,* 2013). According to Barna, (2020), Horizon 2020, which had run from 2014 to 2020, put close attention on climate action and development of clean and efficient energy systems and transports. These effects can be achieved in a micro-turbine system equipped with a heat recovery unit. Gas turbines with output power in 5 to 20kW range are generally classified as micro-turbines (Shah, 2005), and are used extensively in aviation as alternative power units and recently, this technology has found a new application as range extenders in Hybrid electric vehicles. In recent years, micro-turbines have seen increased applications as co-generation and distributed power generation systems. This may partly be attributed to their performance coupled with their compactness and low cost (Design of a Centrifugal Compressor for Micro Gas Turbine). Findings from the studies of (Piancastelli *et al*. (2014), Frizziero *et al.* (2015), Piancastelli *et al.* (2015)) also reported that Radial turbines and compressors are easier to manufacture but face a significant efficiency reduction below 200,000 Re. These factors have drawn more researchers to investigate the miniaturization and optimization of micro-turbines and their components. Despite extensive investigation and research in the micro-turbine niche, the cost of procurement of these systems has barely seen any improvement in the past decade. As pointed out in the study of Adam, (2012), the technology used in micro-turbines is derived from aircraft APUs, diesel engine turbochargers and small jet engines. Similarly, the report from the study of Laurel, (2004) revealed that attempts have been made to derive micro-turbine systems from turbo-chargers. Granted the technological breakthrough in materials engineering and turbocharger technology, the adaptability of a turbocharger for micro-turbine has received a renewed interest among researchers and hobbyists showcasing the feasibility of adapting turbocharger for turbojet application with the generation of up to 75N thrust from adapted automobile turbocharger (Usman, 2019). As pointed out Turbochargers are turbine-driven devices which are commonly integrated with internal combustion engines (ICE), in order to increase the engine inlet air mass flow and pressure (.Luca, 2021) In this study, design procedure framework for the construction of micro-turbine for combined heat and power generation was formulated. The procedural design was achieved using theoretical architecture available in the open literature and its functionality was validated using a numericals simulation approach.

Materials and Methods

Turbine Cycle Modelling

The power cycle modelled for the envisaged microturbine system is a simple Brayton cycle (Figure 1). This process shown in Figure 2a and Figure 2b consists of four stages including Isentropic compression, Constant pressure heat addition, Isentropic expansion and Constant pressure heat rejection for a closed Brayton cycle. The design points consisting of the independent thermodynamic variables and specific turbocharger properties were first considered. These parameters include the ambient pressure P_1, ambient temperature T_1, pressure ratio r_p and compressor and turbines efficiency denoted as η_c and η_t respectively. In addition, the turbine outlet temperature T_4 of 900 K was chosen considering the limit of the current materials.

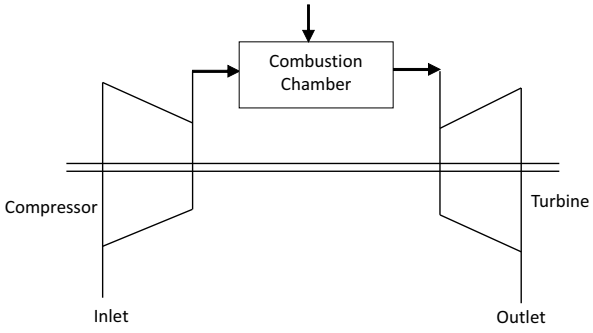

Figure 1: Basic Configuration of a Gas Turbine Engine

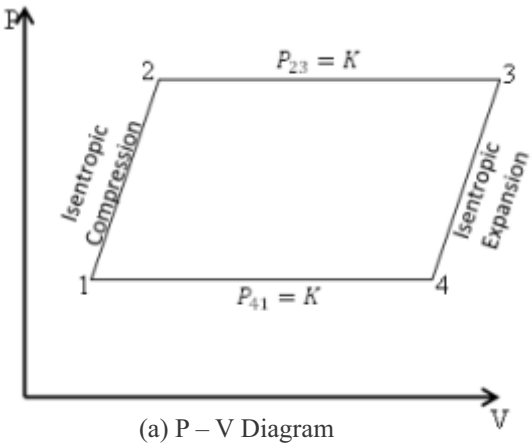

(a) P – V Diagram

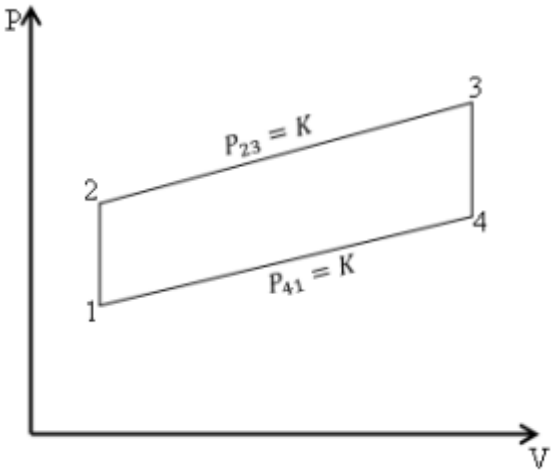

(b) T – S Diagram

Figure 2: Simple Brayton cycle P – V and T – S Diagram

Modelling air as an ideal gas, the compressor outlet temperature was computed using Equation (1)

$$T_2 = T_1\left(1 + \frac{r_p^{\frac{\gamma_a - 1}{\gamma_a}} - 1}{\eta_c}\right) \quad (1)$$

Defining the turbine isentropic efficiency in terms of temperature, the turbine inlet temperature (TIT) was estimated from Equation (2).

$$\eta_t = \frac{T_4 - T_3}{T_3\left(r_p^{\frac{\gamma_a - 1}{\gamma_a}} - 1\right)} \quad (2)$$

From combustor energy balance, the air fuel ratio was obtained using Equation (3):

$$\frac{m_t}{m_a} = \frac{C_{pg}TIT - C_{pa}T_2}{LHV + C_{pf}T_f - (C_{pg}TIT)} \quad (3)$$

The system network outputs were determined using Equations (4) and (5) whilethe theoretical power output was computed from Equation (6).

$$W_c = \frac{c_p T_1\left(r_p^{\frac{\gamma_a - 1}{\gamma_a}} - 1\right)}{\eta_m \eta_c} \quad (4)$$

$$W_t = c_{pg}TIT\frac{\eta_t}{\eta_m}\left(1 - \frac{1}{r_p^{\frac{\gamma_a - 1}{\gamma_a}}}\right) \quad (5)$$

$$P = m_a W_{net} \quad (6)$$

The specific fuel consumption was determined using Equation (7)

$$SFC = \frac{3600}{W_{net}}\frac{m_f}{m_a} \quad (7)$$

A summary of selected and estimated parameters used in the turbine cycle modelling is presented in Table 1.

Table 1: Selected and Estimated Parameters for the Turbine Cycle

Parameter	Value	Unit
Ambient pressure, P_1	101.325	Pa
Ambient temperature, T_1	300	K
Turbine outlet Temperature, T_4	900	K
Compressor pressure ratio, r_c	3	
Compressor efficiency, η_c	≥ 0.75	
Turbine efficiency, η_t	≥ 0.75	
Turbine pressure ratio, r_t	$\frac{1}{3}$	
Compressor outlet temperature, T_2	447.495	K
Turbine inlet temperature, T_3	1096.05	K
Specific heat capacity of fuel (Butane), C_{pf}	1.73	kJ/kg
Mass flow rate of fuel, m_f	0.01	kg/s
Work done by compressor, W_c	157.785	kJ/kg
Work done by turbine, W_t	359.20	kJ/kg
Ne work done, W_{net}	201.415	kJ/kg
Shaft output power, P	60.42	$kWatts$
Specific fuel consumption, SFC	0.61	kg/kWh

Combustor Modelling

The combustor or burner is the component of the microturbine system where combustion takes place. Typically, in gas turbine, air at elevated temperature and pressure is fed into the burner where energy is added at constant pressure. The energized air is subsequently channelled to the turbine where work is done on the system by the high temperature and high pressure air. Among other requirements, the combustor must maintain a smooth, stable and sustained combustion under varying air mass flow rate. To meet the stated requirement, air flowing into the combustor is distributed as primary air and dilution air as pointed out in the study of Keerthana *et al.* (2019) is considered and applied in this study. The design procedure adopted follows the models defined by Lefebvre, (1983). The reference area equivalent of the external combustor casing was determined from Equation (8) as obtained from (Lefebvre, 1983) following the initial design parameters *Uref* chosen between 6.5 - 7 m/s for optimum combustion, density of air *(p3)*at 445K and pressure of 3 bar and has a value of 2.33kg/m^3.

$$A_{ref} = \left[\frac{R}{2}\left(\frac{\dot{m}_3\sqrt{T_3}}{P_3}\right)^2 \frac{\frac{\Delta P_3}{q_{ref}}}{\frac{\Delta P_3}{P_3}}\right]^{0.5} \quad (8)$$

$$q_{ref} = \frac{\rho_3 U_{ref}^{\ 2}}{2} \quad (9)$$

The system flame tube cross-sectional area and diameter are obtained using Equation (10) extracted from the study of Rashid and Elijah (2019) as follow:

$$\frac{A_{ft}}{A_{ref}} = 0.7 \quad (10)$$

The minimum length of flame tube required was estimated from Equation (11) extracted from (Lefebvre, 1983) considering a pattern factor of 2 and transverse quality of 20%.

$$L_{ft} = D_{ft}\left(\frac{A\Delta P_3}{q_{ref}}\ln\left(\frac{1}{1-pf}\right)\right)^{-1} \quad (11)$$

where: A and pf (pattern factor) are constants.The lengths of the primary and secondary zones were obtained from Equations (12) and (13) respectively following Melconian Moldak (1985) recommendation as reported by (Rashid and Elijah, 2019).

Air Mass Flow Rate Distribution

The mass flow rate required at the primary and secondary zones was computed from Equation (14) using an equivalence ratio of 0.9 and 0.7 respectively. The mass flow rate in the dilution zone was obtained as the difference between the net mass flow rate and the mass flow rate at the primary and secondary zones.

$$m = \emptyset(6.5(m_f)) \quad (14)$$

Air Admission Zones

The diameter and number of holes in each zones of mass flow of the combustion chamber are proportional to the mass flow rate of the air jet intended for the section. 60% of the air mass required in the primary zone was designed to be admitted axially through the swirler inlet. The number of holes within the span of the primary zone of the flame tube was evaluated using Equation (15) according to Rashid and Elijah (2019) given as:

$$m_f = \frac{\pi}{4} n d_j^{\ 2} \rho_j U_j \quad (15)$$

The system stream jet diameter *dj* was estimated using Equation (16) and the geometric diameter

$$\frac{Y_{max}}{d_j} = \frac{1.25 j^{0.5} m_g}{m_g + m_j} \quad (16)$$

$$d_h = \frac{d_j}{\sqrt{C_d}} \quad (17)$$

The momentum flux ratio *j* of the system is given by Equation (18), according to (Lefebvre, 1983):

$$j = \frac{\rho_j U_j^{\ 2}}{\rho_g U_g^{\ 2}} \quad (18)$$

2.2.3 Swirler Design

The swirler is a crucial component of the combustor that ensures recirculation and thorough air-fuel mixing. A static vane axial-flow single air swirler was considered for the inlet of the flame tube. For practical air swirler with strong swirls, the swirl number

$$S_N = \frac{2}{3}\left(\frac{1-\left(\frac{D_{isw}}{D_{sw}}\right)^3}{1-\left(\frac{D_{isw}}{D_{sw}}\right)^2}\right)tan\theta \qquad (19)$$

To fulfil the combustion requirement envisaged, 12% of compressed air entering the reference area is channelled axially to the primary zone in the combustion chamber. Thus, the cross sectional area of the required swirler is calculated as follows:

$$\propto_{dome} = cos^{-1}\left[\frac{-D_{ref}(D_{ft}-2D_{sw})(D_{ft}-4L_{rz})\sqrt{D_{ft}^2-4D_{ft}D_{sw}+4D_{sw}^2-8D_{sw}L_{rz}+16L_{rz}^2}}{2D_{ft}^2-4D_{ft}D_{sw}+4D_{sw}^2-8D_{sw}L_{rz}+16L_{rz}^2}\right] \qquad (22)$$

The length of the required dome is calculated using equation (23) as follows:

$$L_{dome} = \frac{D_{ft}-D_{sw}}{2\tan\alpha_{dome}} \qquad (23)$$

A summary of selected and estimated parameters used for the system combustion modelling is presented in Table 2.

Parameter	Value	Unit
Pressure loss factor, q_{ref}	57	
Reference area, A_{ref}	0.0132	m^2
Cross sectional area of the flame tube, $\frac{A_{ft}}{A_{ref}}$	0.7	
Total length of the flame tube, L_{ft}	0.171	M
Mass flow rate into primary zone, m_{pz}	0.0585	kg/s
Mass flow rate into secondary zone, m_{sz}	0.0455	kg/s
Mass flow rate into dilution zone, m_{dz}	0.196	kg/s
Air mass in the primary zone axially, $m_{pz-axial}$	0.0351	kg/s
Velocity of jet in the annulus, U_j	28.7	m/s
Velocity of jet in the annulus, U_g	18.3	m/s
Admission hole properties in the primary zone, j	3.1286	
Maximum penetration depth of air jet, Y_{max}	0.01085	M
Diameter of the admission hole in the primary zone, d_h	0.0103	M
Number of holes in the primary zone, n	7	
Diameter of the admission hole in the secondary zone, d_h	0.01	M
Number of holes in the secondary zone, n	16	
Cross sectional area of the required swirler, A_{sw}	0.00154	m^2
Inner swirler diameter, D_{swin}	0.03	M
Outer swirler diameter, D_{sw}	0.06	M
Swirl number, S_N	0.8	
Swirl vane angle, θ	45.8	°
Divergent angle of dome, α_{dome}	49.53	°
length of required dome, L_{dome}	0.021	m

Heat Exchanger Unit Modelling

The heat exchanger is an integral part of a combined heat and power system. A tube-in-tube heat exchanger is considered in this this study. This is due to its simplicity and relative effectiveness in areas where low pressure luids are concerned. Considering the factors in this work, a heat exchanger with the following specifications in mind is designed in this study: An upper limit of 3kW heat delivery rate is chosen along with the parameters $T_{hin} = 627°C$(expected turbine exit temperature), $T_{cin} = 27°C$(room temperature of water), $T_{cout} = 627°C$(desire final temperature of water). The exit temperature of hot gases from the heat exchanger is calculated using the heat balance equation given in Equation (24) as:

$$m_w c_{pw}(T_{out} - T_{in}) = m_g c_g(T_{hin} - T_{hout}) \quad (24)$$

Mass flow rate of water considered is 0.02kg/s. The expected outlet temperature of water is calculated using the energy quation given in Equation (24) as:

$$m_w c_{pw}(T_{out} - T_{in}) = 3000 \quad (25)$$

A copper tube with an internal diameter of 10.0225cm and thickness 0.29cm was considered for the inner pipe while a copper tube of internal diameter 12.226cm was considered for the outer pipe over several iterative considerations. Thus, the system heat transfer coefficient was obtained using Gnielinski's (1976) correlation for turbulent flow in tubes expressed in Equation (26) as follows:

$$Nu = \frac{\left(\frac{f}{8}\right)(Re - 1000)Pr}{1 + 12.7\left(\left(\frac{f}{8}\right)^{0.5}\left(Pr^{\frac{2}{3}} - 1\right)\right)} \quad (26)$$

where f is the Darcy frictional factor expressed mathematically as:

$$f = 0.76\ (\ln Re - 0.64) \quad (27)$$

The Reynold number of the flue gas in the inner tube was estimated using Equation (28) and the effective length of the tube was determined from Equation (29)

$$R_e = \frac{\rho_g V_g D}{\mu_g} \quad (28)$$

$$L = \frac{\dot{Q} d_{ii} h_{ii} \kappa + \dot{Q} d_{io} h_{io} \kappa + \pi \dot{Q} d_{io} h_{io} d_{ii} h_{ii} \kappa \ln\left(\frac{d_{in}}{d_{ii}}\right)^{\frac{1}{2\pi}}}{\pi \Delta t d_{io} h_{io} d_{ii} h_{ii} \kappa} \quad (29)$$

Where Δt is Logarithmic mean temperature difference, given by Equation (30) for a counter flow heat exchanger; $(T_{hin} - T_{cout})$

$$\Delta t = \frac{-(T_{hout} - T_{cin})}{\ln\left(\frac{T_{hin} - T_{cout}}{T_{hout} - T_{cin}}\right)} \quad (30)$$

The overall heat transfer coefficient U was obtained using Equation (31) as follows:

$$UA = \left(\frac{1}{\pi h_{io} d_{io} L} + \frac{\ln\frac{d_{in}}{d_{ii}}}{2\pi L \kappa} + \frac{1}{\pi h_{ii} d_{ii} L} + R_{in} + R_{out}\right)^{-1} \quad (31)$$

Where A is the heat transfer surface area, obtained as:

$$A = \pi d_{io} L \quad (32)$$

A summary of selected and estimated parameters used for the heat exchanger unit is presented in Table 3.

Table 3: Selected and Estimated Parameters for the System Heat Exchanger Unit

Parameter	Value	Unit
Expected turbine exit temperature, T_{hin}	627	°C
Room temperature of water, T_{cin}	27	°C
Desire final temperature of water, T_{cout}	627	°C
Selected mass flow rate of water, m_w	0.02	kg/s
Outlet temperature of water, T_{cout}	62.71	°C
Outlet temperature of the flue gas, T_{hout}	621.7	°C
Inner Copper tube internal diameter,	10.0225	Cm
Copper tube thickness,	0.29	Cm
Outer copper tube internal diameter,	12.226	Cm
Reynold number of the flue gas in the inner tube, R_e	103,910	
Fictional factor, f	0.008	
Nuselt number, Nu	93.84	
Heat transfer coefficient in the inner pipe, h_i	60.67	W/m^2K
Reynold number in annulus part, R_o	1305.47	
Fictional factor, f	0.008	
Nuselt number, Nu	4.36	
Convective heat transfer coefficient in the annulus, h_o	19.93	W/m^2K
Logarithmic mean temperature difference, Δt	579	°C
Length of the heat exchanger, L	0.285	M
Overall heat transfer coefficient, U	16	W/m^2K

Results and Discussion

The design calculations of the microturbine co-generator components were done through the application of appropriate design equations. Computational fluid dynamic simulation analysis of microturbine co-generator parts was carried out to ascertain the functionality of the system using Solidworks software. The results of the simulation of some of the microturbine co-generator parts are given in Figures. 3 to 6 respectively. The summary of the analytical computation and numerical simulation results obtained are presented in Tables 2 and 3.

Numerical Simulation

The microturbine co-generator onsidered in this study can be divided into three subsystems namely the thermodynamic cycle of the microgas turbine, combustor and heat recovery unit. A design point analysis was carried out using GasTurb13 Trial version to evaluate the thermodynamic cycle based on initial design parameters to enable comparison with the analytical results obtained. The numerical evaluation carried out in this study requires initial inputs or design points including the air mass flow rate, ambient temperature and pressure, turbine inlet temperature, compression ratio and isentropic fficiency of compressor and turbine. Figure 3a and figure 5a show the pressure-volume and temperature-entropy diagram of the envisioned system generated by the software from the inputted design points. Each node on the curves indicates an important point in the cycle, the value of which may significantly alter the overall characteristics of the entire cycle. Node 1-3 in Figure 3a shows the isentropic compression which occurs between the compressor inlet and outlet leading to an increase in density and elevated temperature of air. Node 3-4 as shown in Figures 3a and 5a represent the additionof heat at constant pressure. Node 4-5 on the P-V curve shows the expansion process whereby the energized fluid expands and work is done on the turbine. Presented in Figure 4 are the obtained numerical evaluation results in this study. Table 4 summarizes the results of the software numerical evaluation in comparison with the analytical results.

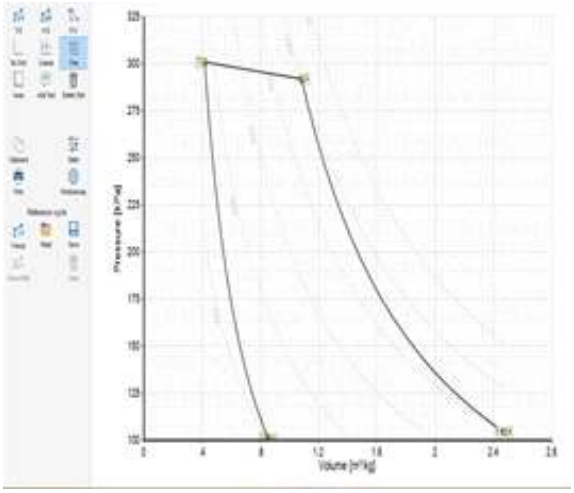

Figure. 3a: Generated P – V Diagram

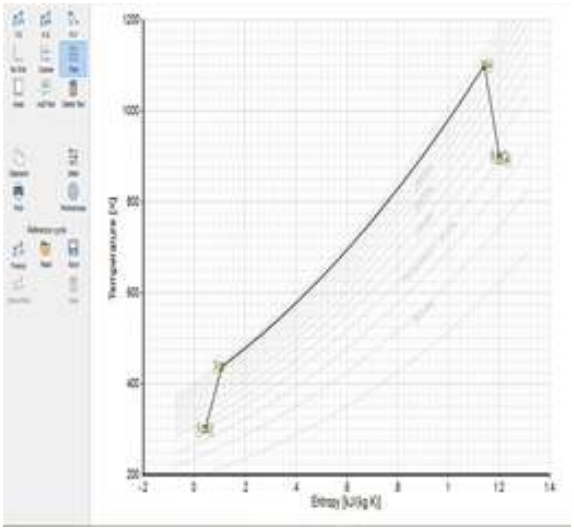

Figure. 3b: Generated T – S Diagram

The results obtained based on analytical computation and numerical simulation of the thermodynamic cycle is summarised in Table 2.

Table 2: Summary of Analytical and Software Validation Results

	Analytical Result	Software Output
Compressor outlet temperature	447K	437.27K
Turbine exit temperature	1096.05K	1096K
Fuel mass flow rate	0.01kg/s	0.01kg/s
Specific fuel consumption	0.61kg/kWh	0.6016kg/kWh
Shaft power	60.42kW	30kW

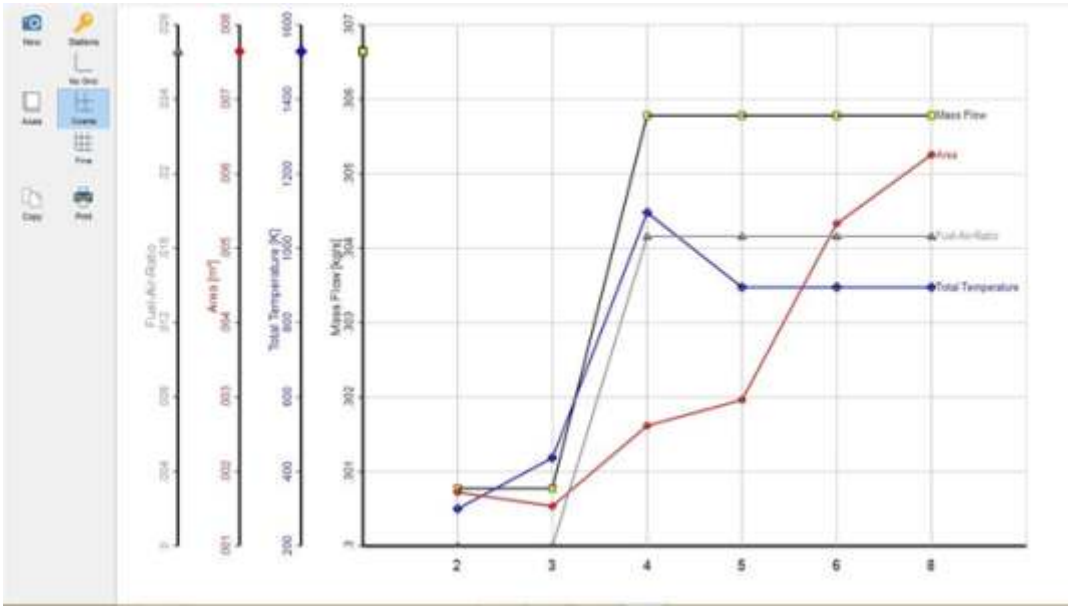

Figure. 4: GasTurb13 Generated Parameters

Simulation of the designed system combustion Unit

The combustor forms the central part of the system in this study. This component determines the performance of the whole system since failure or fault in or around the combustor could render the whole system inoperable. In addition to the results obtained from the analytical design, the combustion process within the combustion chamber was simulated using ANSYS 2021R1 with the geometrical model in simplified 2D form. The 2D model was created in ANSYS workbench Fluent Spaceclaim as a rectangular plane with an equivalent length of the combustion chamber and the width set to an equivalent radius of the combustion chamber to take advantage of the symmetry. An orifice was created 2cm along the axis to prime fuel injection. The planar model was then imported into the Fluent meshing workbench. Edge sizing with 300 divisions was applied along the axis and length boundary. 100 divisions were applied to the air inlet face and 10 divisions were pplied to the fuel inlet. The mesh was further refined with face meshing set to a quadrilateral ethod. The model was imported into the fluent solver and the energy equation was activated. Air and n-Butane were created and assigned as oxidants and fuel respectively. Corresponding boundary conditions were assigned. Specie transport and reaction were used as combustion mechanism. The Solution was initialized using hybrid initialization and the solver was initiated. The temperature and pressure distribution obtained within the combustor are presented in Figures 5a and 5b respectively.

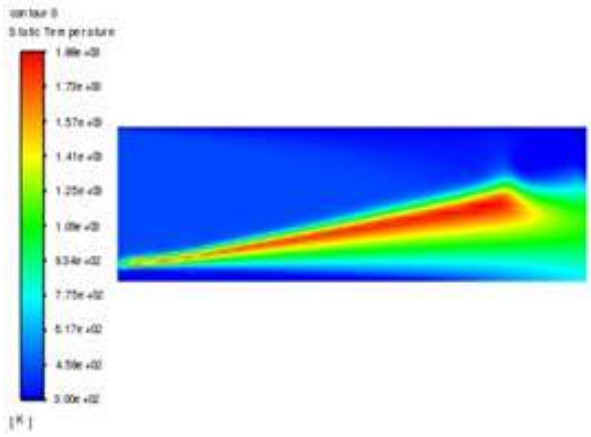

Figure. 5a: Temperature Distribution

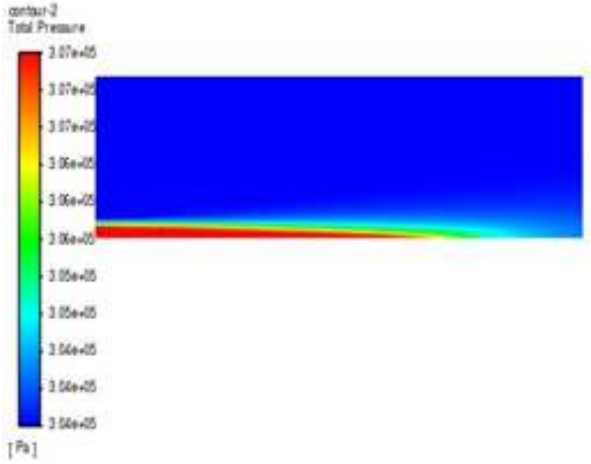

Figure. 5b: Pressure Distribution

Simulation of the Designed System Heat Exchanger Unit

A numerical simulation of the system heat exchanger was similarly carried out using ANSYS 2021R1. A double pipe or pipe-in-pipe heat exchanger was considered. This selection is based on the modularity and effectiveness of the double-pipe heat exchanger in low power applications as it is the case in this study. The result of the analytical design process in this study was validated using ANSYS fluent solver. The procedure involves modelling the heat exchanger based on a delivery power of 3kW and exhaust of the microturbine as hot influx fluid. The 3D model was created using Solidworks software and imported into ANSYS Spaceclaim and refined as shown in Figure 6.The Transient state, k-epsilon model was selected in the solver with gravity effect considered. The corresponding materials (copper, water and flue gas) were assigned to each body. Water was assigned to the fluid body within the annulus while flue gas was assigned to the fluid body in the tube and copper was assigned to solid walls. The inlet temperature was assigned as 900 K for flue gas and 300 K for water. The mass flow inlet of flue gas and water were set to 0.31 kg/s and 0.02 kg/s respectively and the solution was initiated. The result was analysed using the ANSYS fluent post-processing with the analysis restricted to the annulus fluid body domain (water). The simulated result in Figure 6 revealed that the temperature of outflux water volume ranges between 361 K and 367 K within 1.6% of the analytic prediction was attained in this study. It is interesting to point out that the initial results from the analytical design parameter in this study show close agreement with software- generated parameters as in the case of the working cycle. It was also noted that the theoretical predictions obtained for

the heat exchanger closely matched the results of the numerical simulation carried out using ANSYS numerical simulation software with less than a 3% variation in the outlet temperature of the designed system. These variation values are minimal thus implying that the base part is suitable under design condition and it will satisfactorily serve its intended purpose

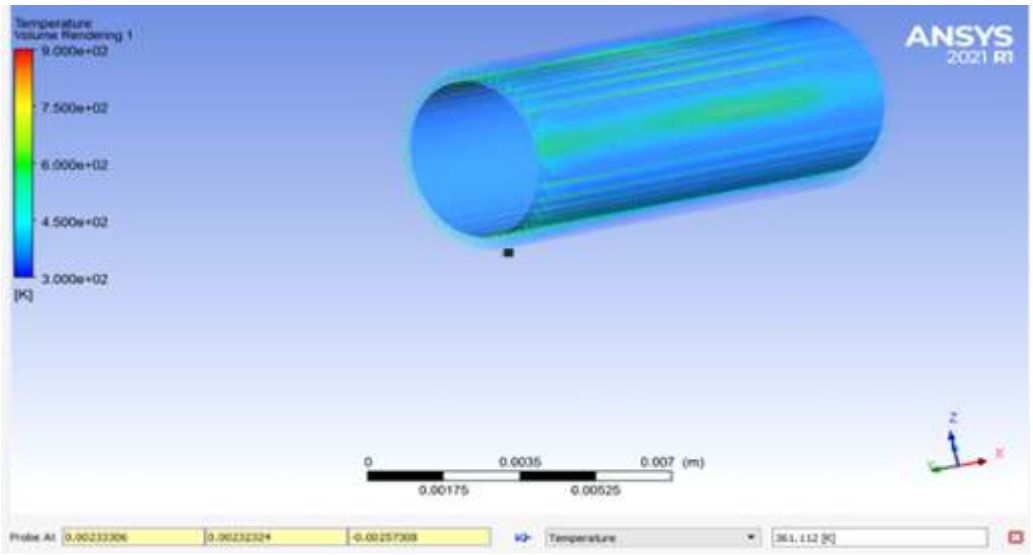

Figure. 6: Temperature Distribution of water in Heat Exchanger

Parameter	Value	Unit
Inlet temperature of exhaust	900	K
Outlet temperature of exhaust	894	K
Inlet temperature of water	300	K
Outlet temperature of water	335	K
Effective length of heat exchanger	0.285	M
Heat transfer surface area	0.092	m^2
Overall heat transfer coefficient	16	$W/m^2/K$

Table 3: Heat Exchanger Characteristics

Conclusion

An Attempt was made in this study to assess the workability of turbine charger-derived microturbine via analytical design and complementary numerical simulation of core components. Results obtained from the analytical design and also corroborated by numerical simulations were based primarily on previously established theoretical framework particularly those of Lefebvre (1983). The close agreement between the results from theoretical computations and those of numerical simulation obtained principally from GasTurb13 for the working cycle at the design stage and ANSYS CFD for the combustion and heat exchanger components unit of the system demonstrate the practicability of a combined heat and power generated system conceived in this study. A numerical simulation software result with less than a 3% variation in the outlet temperature of the designed heat exchanger unit of the system is obtained in this study. These variation values are minimal thus implying that the base part is suitable under design condition and it will satisfactorily serve its intended purpose.

References

Adam, H. (2012). Scaling 3 – 36 kW Microturbines. Conference: Proceedings of ASME Turbo Expo 2012.

Barna, C. (2020), Current Socio-Economic Challenges. Approaching Sustainability and Social Economy, Manag. Dyn. Knowl. Econ., 8(1): 7–9

Frizziero, L.; Rocchi, I.; Donnici, G.; Pezzuti, E. (2015) Aircraft diesel engine turbo compound optimized. JP J. Heat Mass Transf, 11: 133–150.

Gnielinski, V. (1976) New equations for heat and mass transfer in turbulent pipe and channel flow, International Journal of Chemical Engineering. 16 (2): 359-368.

Keerthana C., Anbarasan T., Preethi D., Vairamuthu N. (2019) Design and Analysis of a Combustion Chamber in a Gas Turbine. International Journal of Engineering Research & Technology, 7:1-5

Laurel T. (2004). Design and Performance of Gas Turbine Engine from Automobile Turbocharger. A Bachelor of Science Thesis submitted to Department of Mechanical Engineering, Massachusetts Institute of Technology. 1-46

Lefebvre, A. H. (1983). Gas Turbine Combustion. Washington Hemisphere Pub. Corp., c1983 xvii, 531 p.: ill.; 25 cm.

Luca M. (2021) Performance analysis and dynamics of innovative SOFC hybrid systems based on turbocharger-derived machinery, PhD Thesis, Department of Mechanical, Energy, Management and Transportation Engineering, University of Genoa Polytechnic School, 1-221

Maryam M., MaghankiB., GhobadianG., Najafi R., Janzadeh G.(2013). Micro combined heat and power (MCHP) technologies and applications. Renewable and Sustainable Energy Reviews, 28(C): 510-524.

Manabe, S., (2019) Role of Greenhouse Gas in Climate Change Tellus A Dyn. Meteorol. Oceanogr.71(1): 1620078.

Melconian, J. O and Modak, A. T. (1985). Combustor design. In: SAWYER, JAW. (Ed.) Sawyer's gas turbine engineering handbook design. Volume 1, Theory & design. 3. ed. Connecticut: Turbo machinery International Publications, 1985. v.1, Chapter. 5: 1-5.

Piancastelli, L.; Frizziero, L.; Bombardi, T. (2014) Bézier Based Shape Parameterization in High Speed Mandrel Design. Int. J. Heat Technol. 32: 57–63

Piancastelli, L.; Gatti, A.; Frizziero, L.; Ragazzi, L.; Cremonini, M. (2015) CFD Analysis of the Zimmerman's V173 Stol Aircraft. ARPN J. Eng. Appl. Sci., 10: 8063–8070

Ramon S. and Pedro T. L. (2013). Premliminary Design of a Combustion Chamber for Microtubine based in an Automotive Turbocharger. Proceeding of 22nd International Congress of Mechanical Engineering (COBEM 2013), Ribeirão Preto, SP, Brazil , 412- 421

Rashid S. and Eljah M. (2019). Design and Analysis of Annular Combustion Chamber for a Micro Turbojet Engine. International Journal of Aerospace and Mechanical Engineering, 13: 4-17

Usman B. (2019). Converting an automobile turbocharger into a micro gas turbine. E3S Web of Conferences 95, 02008 (2019), 1-4 https://doi.org/10.1051/e3sconf/20199502008

Shah, R.K. (2005) Compact Heat Exchangers for Microturbines. In Micro Gas Turbines ,**(2–-** 18)